Water Resources Research®

RESEARCH ARTICLE

10.1029/2024WR037333

# Multivariate Evaluation of Flash Drought Across the United States

**Jason A. Otkin[1], Yafang Zhong[1], Trent W. Ford[2], Martha C. Anderson[3], Christopher Hain[4], Andrew Hoell[5], Mark Svoboda[6], and Hailan Wang[7]**

[1]Cooperative Institute for Meteorological Satellite Studies, Space Science and Engineering Center, University of Wisconsin-Madison, Madison, WI, USA, [2]Illinois State Water Survey, Prairie Research Institute, University of Illinois, Champaign, IL, USA, [3]Hydrology and Remote Sensing Laboratory, USDA-ARS, Beltsville, MD, USA, [4]NASA Marshall Space Flight Center, Earth Science Branch, Huntsville, AL, USA, [5]NOAA Physical Sciences Laboratory, Boulder, CO, USA, [6]National Drought Mitigation Center, University of Nebraska-Lincoln, Lincoln, NE, USA, [7]NOAA Climate Prediction Center, College Park, MD, USA

**Key Points:**

- A multivariate climatology of flash drought onset and severity is created for the United States using several drought indicators
- Flash drought occurrence and severity varied with season and region and the indicator used to identify flash drought events
- The strongest flash droughts when evaluated using a multivariate perspective occurred in the central and southeastern United States

**Correspondence to:**

J. A. Otkin,
jasono@ssec.wisc.edu

**Citation:**

Otkin, J. A., Zhong, Y., Ford, T. W., Anderson, M. C., Hain, C., Hoell, A., et al. (2024). Multivariate evaluation of flash drought across the United States. *Water Resources Research*, *60*, e2024WR037333. https://doi.org/10.1029/2024WR037333

Received 22 FEB 2024
Accepted 5 OCT 2024

**Abstract** This study uses the flash drought intensity index (FDII) to develop a multivariate flash drought climatology for the contiguous U.S. using data from 2001 to 2021. The FDII method uses the rate of intensification (FD-INT) and subsequent drought severity (DRO-SEV) to determine when a flash drought occurred and the strength of the event. Overall, the results showed that flash drought occurrence and severity varied with season and region and were sensitive to the drought indicator used to compute the FDII. Precipitation-based indicators identified more flash droughts across the western U.S. whereas soil moisture (SM) and evapotranspiration indicators identified more flash droughts across the central and eastern U.S. When assessed over the entire U.S., the most flash droughts were found when using an evaporative demand indicator. Though FD-INT was larger than DRO-SEV across the U.S. for most indicators, regional patterns were also evident in their relative importance. For example, a distinct east-west gradient was present in the SM and evapotranspiration FD-INT, with relatively large values in the central and eastern U.S. A combined data set synthesizing information from multiple indicators showed that the strongest flash droughts from a multivariate perspective were located in the central and southeastern U.S. A seasonal analysis revealed a distinct seasonal cycle in flash drought onset across the western and central U.S. Together, the results illustrate the need to use a multivariate framework to identify and characterize the occurrence and severity of flash droughts.

**Plain Language Summary** Flash droughts are characterized by rapid intensification leading to sustained drought conditions that impact natural and human ecosystems. This study used several drought monitoring data sets to develop a multivariate flash drought climatology for the contiguous U.S. that captures both when flash droughts occur and their severity. Overall, the results revealed that flash drought occurrence and severity varied with season and region and were sensitive to the indicator used to characterize these events. Precipitation-based indicators identified more flash droughts across the western U.S. while SM and evapotranspiration indicators identified more flash droughts across the central and eastern U.S. When assessed over the entire U.S., the most flash droughts were identified when using an indicator of evaporative demand. A combined indicator that synthesizes information from multiple indicators showed that the strongest flash droughts were located in the central and southeastern U.S. A seasonal analysis revealed a distinct seasonal cycle in flash drought occurrence across the western and central U.S. Together, the results illustrate the need to use a multivariate analysis framework to identify and characterize the severity of flash droughts.

## 1. Introduction

Flash droughts have garnered substantial research interest during the past decade given their large impacts (Christian et al., 2024). These events are characterized by unusually rapid intensification over a short period of time relative to climatological expectations for a given location and time of year (Otkin et al., 2018, 2022; Svoboda et al., 2002). Conceptually, flash droughts reside at the intersection of rapid intensification (e.g., the "flash" component) and the presence of insufficient water resources to meet the needs of the natural or human environment (e.g., the "drought" component). This combination of factors differentiates flash droughts from short periods of dry weather that do not lead to drought and from conventional droughts that develop more slowly. Lisonbee et al. (2021) note that many quantitative definitions have been developed to detect flash droughts based on variables depicting anomalies in atmospheric or land surface conditions. Most definitions have been designed to identify flash droughts using a set of thresholds requiring a minimum rate of intensification over a specified period of time (Chen et al., 2019; Christian et al., 2019; Ford & Labosier, 2017; Li et al., 2020; Liu et al., 2020; Mishra et al., 2021; Nguyen et al., 2019; Noguera et al., 2020; Osman et al., 2021; Parker et al., 2021; Pendergrass et al., 2020). Because such definitions only account for one of the factors described above (rapid intensification), Otkin et al. (2021) developed the flash drought intensity index (FDII) to account both for the rapid rate of intensification and the subsequent drought severity (DRO-SEV). The FDII is useful for characterizing flash droughts because it provides a more complete measure of their severity than existing methods that only consider the rate of intensification.

Flash drought is a compound climate event (Zscheischler et al., 2018) characterized by multiple meteorological drivers and environmental impacts that may cascade with time. Rapid drought intensification is more likely to occur when high temperatures, low relative humidity, strong winds, and sunny skies combine to enhance atmospheric evaporative demand (Otkin et al., 2013). Rapid moisture depletion can occur at the land surface due to increased transpiration from vegetation and insufficient rainfall to replenish soil moisture (SM). Koster et al. (2019) has shown that large precipitation deficits are an important driver of flash drought; however, flash droughts can also develop with near normal precipitation if the evaporative demand is large (Christian et al., 2021). Variables such as SM, evapotranspiration (ET), vegetation health, evaporative demand, and precipitation are typically used to identify flash droughts (Lisonbee et al., 2021) because they capture the primary drivers and impacts associated with these events. Otkin et al. (2022) noted that flash drought monitoring tools should include multiple meteorological and land surface variables, such as those listed above, to promote a more comprehensive assessment of flash drought evolution in space and time. They also noted that it could be beneficial to generate a measure of consensus regarding the presence and severity of flash drought using multiple variables. In a comparison of flash drought indicators representing a variety of definitions and processes, Ford et al. (2023) found that no single indicator consistently performed the best at identifying flash drought events across the U.S. The regional sensitivity of their results to the indicators being used supports the argument for using a multivariate framework to monitor flash droughts.

In this study, we use a modified version of the FDII and a set of commonly used drought monitoring indicators to assess flash drought characteristics across the contiguous U.S. Because a single indicator is unable to represent all aspects of a flash drought, we assume that each indicator represents a version of the truth and that together they can be used to more comprehensively evaluate flash drought characteristics (Osman et al., 2021). A convergence of evidence approach can be used to provide greater confidence of flash drought hot spots, as well as the severity and seasonality of flash drought. The occurrence of many noteworthy flash droughts around the world in recent decades (e.g., Christian et al., 2020; Hoell et al., 2020; Hunt et al., 2021; Liang et al., 2023; Nguyen et al., 2021; Otkin et al., 2016; Parker et al., 2021; Wang & Yuan, 2021) and the potential for flash droughts to become more common due to climate change (Christian et al., 2023; Mahto & Mishra, 2023; Yuan et al., 2023) demonstrate the need to continue to expand our knowledge of this important climate phenomenon. The paper is organized as follows. The drought indicators are described in Section 2 and then the FDII is described in Section 3. Results are shown in Section 4, with a discussion in Section 5, and the conclusions and future work described in Section 6.

## 2. Drought Monitoring Indicators

Many indicators have been used to assess the characteristics of flash droughts. These indicators are broadly categorized as representing SM, evaporative demand, ET, precipitation, and expert analyses such as the United States Drought Monitor (USDM; Svoboda et al., 2002). For this study, at least one indicator from each category, along with a multivariate indicator that combines information from these indicators, are used to detect and characterize flash drought events. Each indicator is described in greater detail in this section. The drought indicators chosen for this study are selected based on their widespread use in previous flash drought studies and their availability for operational drought monitoring purposes. The study area covers the contiguous United States (Figure 1).

### 2.1. Soil Moisture

SM conditions in the 0–40 cm layer are represented using the Noah land surface model (Barlage et al., 2010; Ek et al., 2003; Wei et al., 2013) that is part of the second North American Land Data Assimilation System (NLDAS-

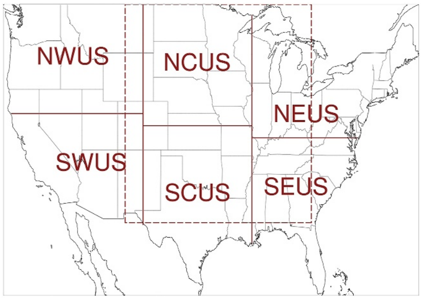


**Figure 1.** Map showing the study area over the contiguous United States. The geographic extent of the 2012 flash drought case study in Section 4.1 is indicated by the dashed lines whereas the solid lines depict the boundaries of the six regions used in the regional analysis in Section 5.

2; Xia et al., 2012). This layer was chosen as a compromise between the fast, but potentially noisy, response of topsoil moisture (0–10 cm) to precipitation and the slower evolution of SM when evaluated over deeper layers (0–200 cm). Hourly SM with 0.125° horizontal resolution from 1979 to 2021 were used to create 28-day averages at weekly intervals and then standardized SM anomalies with a mean of zero and standard deviation of one were computed using these averages. Data from the Noah model was chosen because prior studies (Ford & Quiring, 2019; Xia et al., 2012) have found that it has high fidelity with in situ SM observations. A 28-day period was used to compute anomalies in SM (and all other variables) to lessen the impact of wetting/drying cycles associated with small rainfall events that can make it challenging to use shorter averaging periods such as pentads to detect flash droughts.

### 2.2. Evaporative Demand Drought Index

Anomalies in atmospheric evaporative demand are represented using the Evaporative Demand Drought Index (EDDI; Hobbins et al., 2016). EDDI is a nonparametric method that estimates evaporative demand via the Penman-Monteith equation and an inverse normal approximation to derive the probability distribution at a grid point. Positive (negative) values indicate that the evaporative demand is above (below) the climatological median for a given location, averaging period, and time of year. For this study, 28-day EDDI anomalies covering the contiguous U.S. with 0.125° resolution were obtained from the NOAA Physical Sciences Laboratory (https://psl.noaa.gov/eddi/). This version of EDDI estimates evaporative demand using data from NLDAS-2, with the standardized anomalies computed using data from 1979 to 2015.

### 2.3. Evaporative Stress Index

The Evaporative Stress Index (ESI) is an ET-based drought monitoring tool that represents standardized anomalies in reference ET fraction ($ET/ET_{ref}$), where the Atmosphere Land Exchange Inverse (ALEXI; Anderson et al., 1997, 2007a, 2007b) model is used to estimate actual ET and $ET_{ref}$ is computed using the Penman-Monteith equation (Allen et al., 1998). Use of a reference ET limits the influence of non-soil-moisture drivers of ET, such as solar radiation or the seasonal cycle in evaporative demand, thereby leading to more useful information about SM impacts on plant health. ALEXI estimates the latent, sensible, and ground heat fluxes using the Norman et al. (1995) two-source energy balance model and land surface temperatures from satellite infrared imagery. The total surface energy budget for a given satellite pixel is estimated using the increase in land surface temperature during the morning when the planetary boundary layer is actively growing. Because thermal-based ET retrievals can only be computed when skies are clear, daily clear-sky ET estimates are composited over multi-week periods to obtain more complete coverage (Anderson et al., 2007b). For this study, 28-day ESI anomalies covering the contiguous U.S. with 0.125° spatial resolution are computed each week using data from 2001 to 2021.

### 2.4. Precipitation Indicators

Departures in precipitation and near-surface water balance were assessed using existing daily gridded 30-day Standardized Precipitation Index (SPI; McKee et al., 1993) and Standardized Precipitation Evapotranspiration Index (SPEI; Vincente-Serrano et al., 2010) analyses available from gridMET (Abatzoglou, 2013), which is a hybrid observational data set that combines input from the NLDAS and Parameter-elevation Regressions on Independent Slopes Mode (PRISM; Daly et al., 2008) data sets. The SPI is computed using precipitation data whereas the SPEI accounts for both precipitation and temperature by assessing differences between precipitation and reference ET. The SPI and SPEI were standardized using data from 1979 to 2022. This study uses SPI and SPEI analyses at weekly intervals that were upscaled from their native 4-km resolution to the 0.125° resolution grid used by the other indicators. A negative (positive) SPI indicates that the precipitation for a given location was less (more) than the climatological median precipitation over the 30-day period. Likewise, a negative (positive) SPEI indicates a 30-day surface water deficit (surplus) relative to climatology for that location and time period.

10.1029/2024WR037333

### 2.5. United States Drought Monitor

The USDM is created each week by a team of experts that synthesize numerous inputs such as precipitation, snowpack or snow water equivalent, SM, crop and range conditions, streamflow, reservoir levels, and local impacts to produce a best estimate of DRO-SEV (Svoboda et al., 2002). Though the process is designed to be objective, there is still some subjectivity because only a single DRO-SEV can be assigned at a given location each week even though there may be differences in DRO-SEV among the various indicators and impact reports being used. The weekly USDM analyses depict abnormally dry conditions (D0), along with four drought categories including moderate (D1), severe (D2), extreme (D3), and exceptional (D4) drought, as well as locations that are free of drought. This study uses weekly USDM analyses updated each Tuesday from 2001 to 2021. It is important to note that the number of data sets and impact reports used to construct the weekly USDM analyses has changed during the USDM period of record. Though an improved representation of flash drought has likely occurred during the past decade because of increased awareness of flash drought, we have chosen to retain the full USDM period of record because precipitation and temperature, which are important drivers of flash drought, have always been key inputs to the USDM.

### 2.6. Combined Flash Drought Indicator

Due to the multivariate nature of flash drought, a combination (COMB) flash drought indicator is also calculated using the FDII computed separately for the SPI, SPEI, EDDI, ESI, and SM variables (see the next section for a description of the FDII). The USDM is not included because it is a categorical indicator rather than a continuous variable. The COMB FDII for a given grid point and week is computed as the mean of the FDII for these five variables, but is set to zero if only one of the variables indicates flash drought.

### 2.7. Indicator Standardization

All indicators were standardized to have a mean of 0 and a standard deviation of 1 and then used to compute the FDII. The indicators are derived using different approaches, both parametric and non-parametric, and these differences could affect their comparability and their depiction of individual flash droughts or climatological flash drought characteristics. However, flash drought studies, whether based on historical or projected climate information, often use different methods to identify flash drought, even if using the same variable. Likewise, the many operational products used for national or global drought monitoring have different methods to identify and characterize drought. Therefore, we acknowledge differences in drought indicator derivation as a caveat to the study results.

## 3. Methods

### 3.1. Flash Drought Intensity Index

The occurrence and severity of flash drought events across the contiguous U.S. from 2001 to 2021 are determined using the FDII framework introduced by Otkin et al. (2021). Their study characterized flash droughts by tracking changes in percentiles over pentad (5-day) time scales; however, this study employs a modified version of the FDII that employs standardized anomalies computed over weekly time steps to align with the weekly cadence of drought analyses from the USDM. Standardized anomalies are used to characterize the DRO-SEV and intensification because their unbounded range is better able to represent the magnitude of extreme climate events such as flash drought (Anderson et al., 2007a, 2007b).

For all data sets, except for the USDM, standardized change anomalies are used to depict how quickly conditions are changing over various time scales (Otkin et al., 2013). Standardized change anomalies, denoted as $\Delta v$, are computed for a given variable by differencing the 28-day (ESI, EDDI, SM) and 30-day (SPI, SPEI) values over 2, 3, …, 7-week time periods:

$$\Delta v(w_1, w_2, y) = \frac{(v(w_2, y) - v(w_1, y)) - \frac{1}{ny}\sum_{y=1}^{ny}(v(w_2, y) - v(w_1, y))}{\sigma(w_1,\ w_2)}, \quad (1)$$

10.1029/2024WR037333

where $v$ is the variable being time differenced, $w_1$ and $w_2$ are the 2 weeks used to compute the difference, $y$ is the year, $ny$ is the number of years, and the denominator is the standard deviation of the differences. By using a range of time differencing intervals to compute the standardized change anomalies, it is possible to assess drought intensification rates across various time scales relevant to flash drought development. Large anomalies show that conditions are rapidly changing relative to average conditions for that location and time of year. Standardizing the changes rather than simply using raw differences from 1 week to the next means that the method can account for local variability in drought intensification rates.

As described in Otkin et al. (2021), the FDII includes two components: one that represents the intensification rate (FD-INT) and another that measures the DRO-SEV. The intensification rate and DRO-SEV components are computed relative to baseline thresholds that signify the minimum requirements for flash drought. We require a baseline intensification rate equivalent to a standardized change anomaly of −0.85 (ΔCHA-BASE) over a 3-week period (ΔT-BASE), which means that the changes fall below the 20$^{\text{th}}$ percentile of a normal distribution. For the USDM, we require the equivalent of a minimum 2-category degradation over a 6-week period. These thresholds were chosen so that only the largest changes are considered to be flash drought, and are consistent with prior studies (e.g., Nguyen et al., 2023; Pendergrass et al., 2020). The intensification component for a given week and grid point is computed as:

$$\text{FD-INT} = \left(\frac{\Delta\text{CHA-BASE}}{\Delta\text{T-BASE}}\right)^{-1} \cdot \left(\frac{\Delta\text{CHA-OBS}}{\Delta\text{T-OBS}}\right)_{\max} \tag{2}$$

where the first term represents the inverse of the baseline intensification rate (which is a constant) and the second term is the maximum intensification rate determined by searching for the maximum intensification rate during the previous 2, 3, 4, 5, 6, and 7 week periods ending at the analysis time. This process is repeated for each indicator. By assessing changes over a range of time scales, the FDII framework can better represent the maximum intensification rate at a given grid point. This flexible analysis framework allows us to identify flash drought events and assess their severity. When scaled by the baseline intensification rate, the magnitude of the changes required for an event to be considered a flash drought increase for longer differencing periods, ranging from a minimum intensification rate of −0.57 standardized change anomalies over a 2-week period to −1.98 standardized anomalies over a 7-week period. For the USDM, the minimum intensification rate varies from a 2-category degradation for differencing periods spanning 2–6 weeks to a 3-category degradation for a 7-week period. For a given variable, FD-INT is set to zero when the temporal change does not exceed the baseline intensification rate. Figures 2a and 2b show the FD-INT over a range of intensification rates for the continuous and categorical variables.

After computing FD-INT, the next step is to calculate the DRO-SEV. Similar to Otkin et al. (2021), the average DRO-SEV is calculated using data from the 13 weeks after the rapid intensification period ends. This duration was chosen because flash drought, as a sub-seasonal water resources phenomenon, transitions into longer-term drought when drought conditions persist beyond 13 weeks. To ensure a similar range of values is possible for all indicators, slightly different formulas are used for the USDM and non-categorical (e.g., ESI, etc.) indicators. For the non-categorical indicators, DRO-SEV is computed as:

$$\text{DRO-SEV} = 1 + \frac{1}{\text{nw}}\sum_{n=1}^{nw}(\text{DRO-BASE} - \text{DRO-OBS}(n)) \tag{3}$$

and for the USDM as:

$$\text{DRO-SEV} = \sqrt{\frac{1}{nw}\sum_{n=1}^{nw}(\text{DRO-BASE} - \text{DRO-OBS}(n))} \tag{4}$$

where $nw$ is the number of weeks, DRO-OBS($n$) is the standardized anomaly for week $n$ for the non-categorical variables or the negative of the drought category for the USDM, and DRO-BASE is the baseline drought threshold. For the non-categorical variables, DRO-BASE is set to −0.85 (the 20th percentile of a normal distribution), whereas for the USDM, it is set to 0 as that corresponds to the abnormally dry (D0) category. For a

Standardized Anomalies

| (a) DT_OBS \ DCHA_OBS | -0.85 | -1.00 | -1.25 | -1.50 | -1.75 | -2.00 |
|---|---|---|---|---|---|---|
| 2 weeks | 1.50 | 1.76 | 2.21 | 2.65 | 3.09 | 3.53 |
| 3 weeks | 1.00 | 1.18 | 1.47 | 1.76 | 2.06 | 2.35 |
| 4 weeks | 0.00 | 0.00 | 1.10 | 1.32 | 1.54 | 1.76 |
| 5 weeks | 0.00 | 0.00 | 0.00 | 1.06 | 1.24 | 1.41 |
| 6 weeks | 0.00 | 0.00 | 0.00 | 0.00 | 1.03 | 1.18 |
| 7 weeks | 0.00 | 0.00 | 0.00 | 0.00 | 0.00 | 1.01 |

FD_INT (0, 1, 2)

U.S. Drought Monitor

| (b) DT_OBS \ DCHA_OBS | 2 | 3 | 4 | 5 |
|---|---|---|---|---|
| 2 weeks | 3.00 | 4.50 | 6.00 | 7.50 |
| 3 weeks | 2.00 | 3.00 | 4.00 | 5.00 |
| 4 weeks | 1.50 | 2.25 | 3.00 | 3.75 |
| 5 weeks | 1.20 | 1.80 | 2.40 | 3.00 |
| 6 weeks | 1.00 | 1.50 | 2.00 | 2.50 |
| 7 weeks | 0.00 | 1.29 | 1.71 | 2.14 |

FD_INT (0, 2, 4, 6, 8)

DRO_BASE -0.85

| (c) DRO_OBS | -0.85 | -1.00 | -1.25 | -1.50 | -1.75 | -2.00 |
|---|---|---|---|---|---|---|
| DRO_SEV | 1.00 | 1.15 | 1.40 | 1.65 | 1.90 | 2.15 |

DRO_SEV (1, 1.5, 2, 2.5)

DRO_BASE 0

| (d) DRO_OBS | -1 | -2 | -3 | -4 |
|---|---|---|---|---|
| DRO_SEV | 1.00 | 1.41 | 1.73 | 2.00 |

DRO_SEV (1, 1.5, 2, 2.5)

**Figure 2.** (a–b) Charts showing the variation of the FD-INT term as a function of the observed intensification rate for the continuous and categorical drought monitoring indicators. ΔT_OBS and ΔCHA_OBS denote the time differencing interval and change in the indicator over that time interval used to compute the observed intensification rate. Combinations that do not exceed the baseline intensification rate for a given time differencing interval are set to zero. (c–d) Charts showing the variation of the drought severity (DRO-SEV) term as a function of the observed DRO-SEV averaged over a 13-week period (DRO-OBS) for the continuous and categorical indicators.

given variable, the observed DRO-SEV must remain below DRO-BASE for a minimum of four consecutive weeks for the event to be classified as a flash drought. This threshold was chosen to eliminate short periods of dryness that are unlikely to lead to large impacts on the land surface. If DRO-OBS($n$) > DRO-BASE for a given week, the incremental DRO-SEV for that week is set to 0. By doing this, the DRO-SEV can be assessed over a longer time frame, with DRO-SEV becoming larger the longer drought conditions persist or the more severe they become (Figures 2c and 2d).

Finally, the observed intensification rate and DRO-SEV for a given grid point and week are used to compute the intensity of the flash drought:

$$\text{FDII} = \text{FD-INT} * \text{DRO-SEV} \tag{5}$$

In its current design optimized for climatological flash drought studies, the FDII is both backward and forward looking because there must be both ongoing rapid intensification and a subsequent period of sustained drought conditions for it to be nonzero on any given week. This means that the date of the weekly FDII could be assigned to be either the junction between the individual time periods used to compute FD-INT and DRO-SEV or to be the end of the time period used to calculate DRO-SEV. Because flash droughts are distinguished by rapid intensification, we use the junction date because that date corresponds to when rapid intensification is occurring.

## 4. Results

### 4.1. 2012 United States Flash Drought Example

The FDII methodology is used in this section to examine the multivariate characteristics of the 2012 U.S. flash drought (see Figure 1 for study area). Figure 3 illustrates the method by showing the evolution of the FD-INT, DRO-SEV, and FDII variables computed using SM at bi-weekly intervals from 09 May to 01 August 2012. On 09 May, FD-INT indicates that conditions were rapidly deteriorating across much of the south-central U.S., with

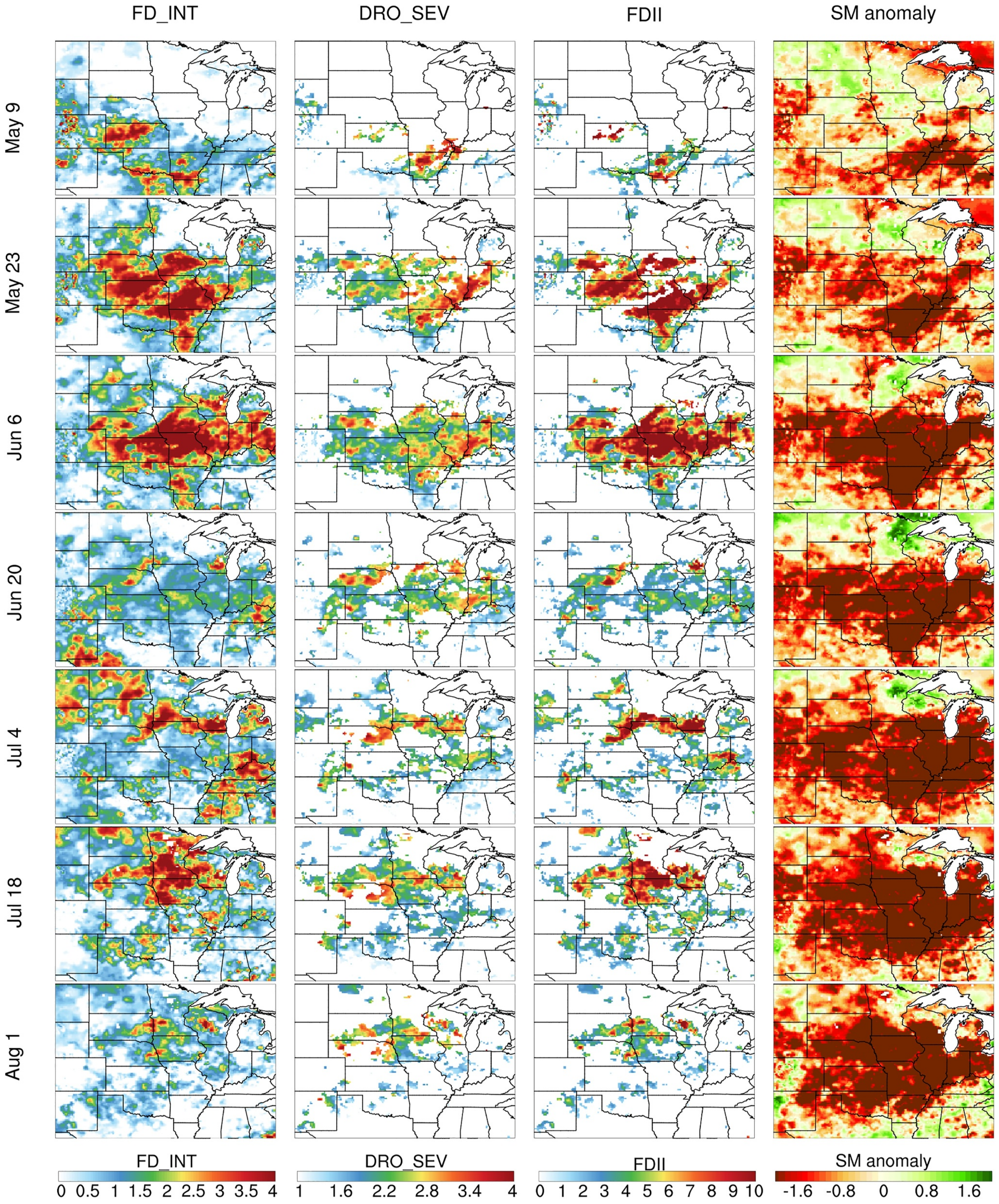


**Figure 3.** Evolution of the FD-INT, drought severity, and flash drought intensity index (columns 1–3) computed using the soil moisture (SM) indicator at 2-week intervals from 09 May to 01 August 2012. The 4-week SM anomalies for each date are shown in column 4.

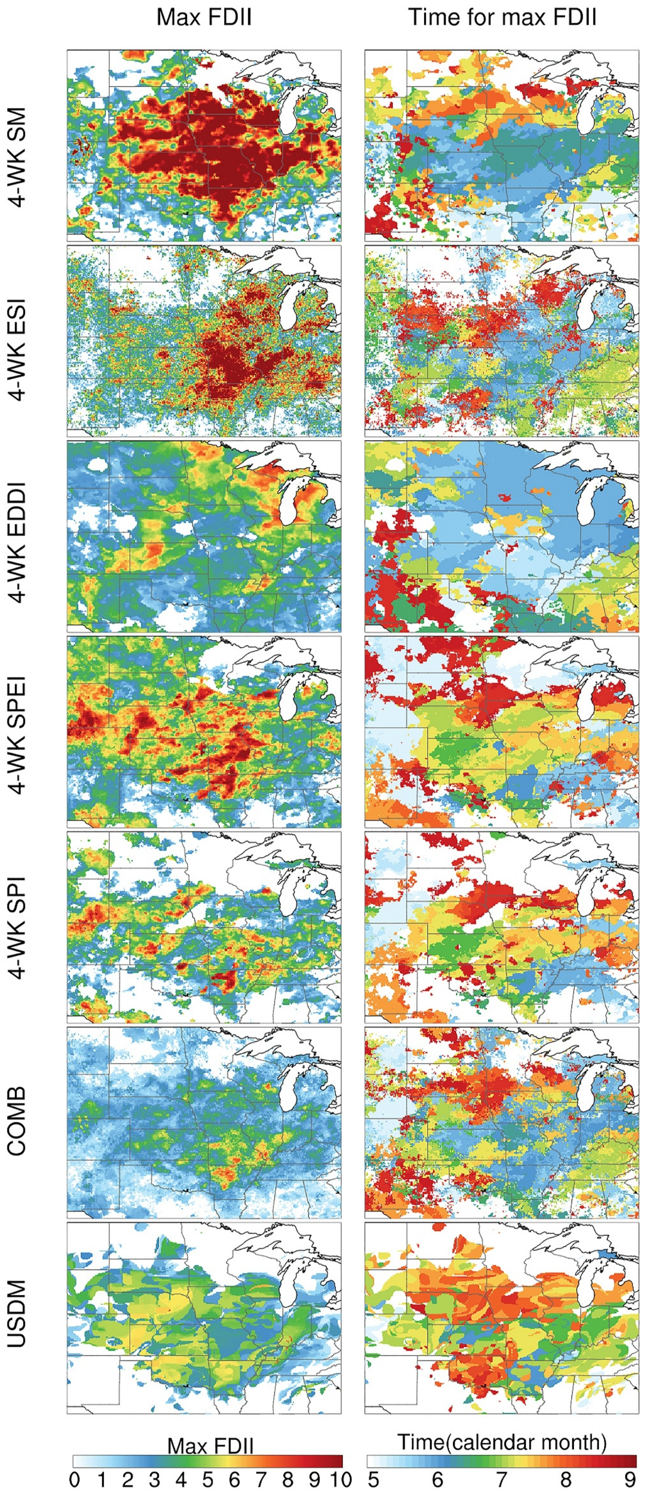


**Figure 4.** Maximum flash drought intensity index (FDII) (left column) and timing of the maximum FDII (right column) for the soil moisture, Evaporative Stress Index, SPEI, EDDI, SPI, COMB, and USDM indicators computed using weekly data from 01 May to 18 August 2012.

large FD-INT spreading across a larger region by 06 June. The spatial extent of FDII is smaller than indicated by FD-INT because drought conditions (SM < −0.85) had not yet developed in some locations, which illustrates the importance of requiring drought conditions to be present for it to be considered a flash drought. The spatial coverage of the FDII was maximized on 06 June because that date corresponds to when both rapid intensification and actual drought conditions were most widespread across the region. After this initial surge of flash drought onset in June, new areas of flash drought developed further north during July as severe drought became entrenched across much of the region.

To more closely examine the multivariate characteristics of this event, Figure 4 shows the magnitude and date of maximum FDII between 01 May and 18 Aug for the SM, ESI, SPEI, EDDI, SPI, COMB, and USDM. Consistent with the evolution of the SM FDII in Figure 3, all indicators except for EDDI exhibit a general northward progression of the maximum FDII with time. Notable differences in the timing of the maximum FDII occurred however with the largest EDDI, ESI, and SM FDII values from Kansas eastward to Michigan occurring from late May to early June whereas they occurred several weeks later in the SPI, SPEI, and USDM. The EDDI (USDM) indicators generally have the earliest (latest) maximum FDII during this event. The COMB indicator shows that the flash drought started in the mid-Mississippi River Valley in early May and then spread northwestward during the next few months. An exception is the High Plains from Colorado to Montana where the maximum COMB FDII occurred in early May due to the influence of very warm and dry weather during the spring (Hoerling et al., 2014) on the SPI, SPEI, and EDDI. Areas further east also experienced warm and dry conditions during the spring but did not experience flash drought according to the FDII because the respective indices were still above the DRO-SEV threshold used to define drought. Moreover, the later occurrence of the maximum FDIIs in the ESI and SM despite the unusually warm spring temperatures reflects the inactivity of vegetation and minimal demands on SM during that time of the year. These results are broadly similar to those shown in Mohammadi et al. (2022) using a solar-induced chlorophyll fluorescence data set that provides information about photosynthesis.

Comparison of the maximum FDII between indicators also reveals large differences in spatial extent and magnitude. For example, indicators such as the SM, ESI, and SPEI depicting land surface conditions contain large areas with FDII >6 whereas meteorological quantities such as SPI and EDDI have smaller maximum FDIIs across most of the region. These results show that indicators more directly representative of conditions at the land surface experienced especially rapid intensification and DRO-SEV when compared to the meteorological drivers. One of the reasons for this behavior is that it is more difficult for a location to experience unusually rapid decreases (increases) in rainfall (temperature) over several weeks that are then maintained for at least three additional weeks because even a short period of cooler weather or a moderate rainfall event can have a strong impact on EDDI and SPI. The land surface variables in contrast integrate the impact of the meteorological drivers over a longer time period and are therefore less sensitive to short periods of cooler weather or small rainfall events. COMB shows that flash drought occurred across a large area, with FDII maximized across the mid-Mississippi River Valley where all indicators except for EDDI had large FDII. The spatial extent of the COMB FDII is very similar to that shown

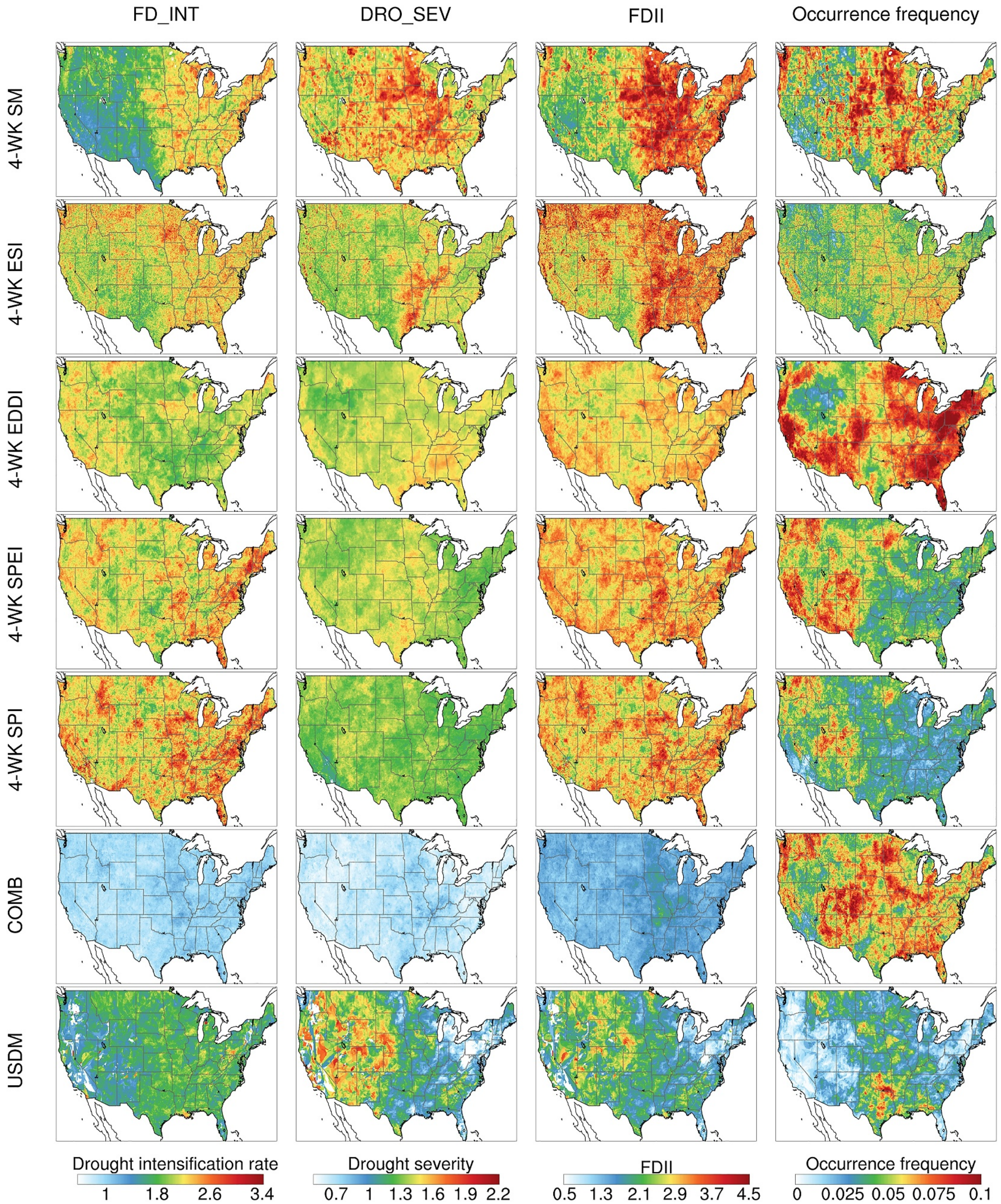


**Figure 5.** Mean FD-INT, drought severity, and flash drought intensity index (FDII) values (columns 1–3) computed using all weeks with a non-zero FDII (column 4) during the 2001–2021 growing seasons (April–October). Results are shown for the soil moisture, Evaporative Stress Index, SPEI, EDDI, SPI, COMB, and USDM.

by the USDM, though there are some differences in the timing of the maximum FDII across the eastern part of the region. Together, the results shown in this section illustrate the need to use more than one indicator to evaluate flash drought characteristics.

### 4.2. Multivariate Flash Drought Climatology

To develop a multivariate climatology of flash drought occurrence and severity across the contiguous U.S., the FDII method was applied to the SM, ESI, SPEI, EDDI, SPI, COMB, and USDM. The climatology uses weekly data from 2001 to 2021, focusing on the warm season (April to October) when vegetation is actively growing. Figure 5 shows the frequency of weeks when the FDII is >0 along with the mean FD-INT, DRO-SEV, and FDII

10.1029/2024WR037333

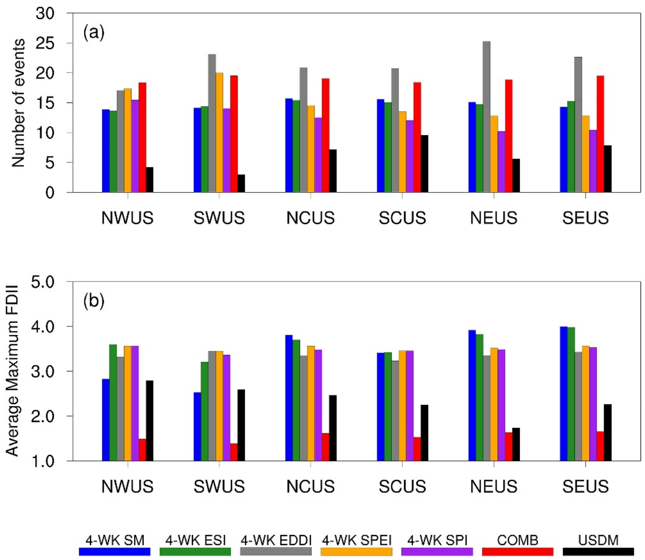


**Figure 6.** (a) Number of flash drought events and their (b) maximum flash drought intensity index averaged across all land grid points for the soil moisture, Evaporative Stress Index, SPEI, EDDI, SPI, COMB, and USDM. Results are computed using weekly data from the 2001–2021 growing seasons (April–October) for the NWUS, SWUS, NCUS, SCUS, NEUS, and SEUS regions.

for each grid point computed using data from those weeks. Overall, FD-INT is larger than DRO-SEV across most of the U.S. in most indicators. Regional patterns are also evident in each variable. For example, SM FD-INT has a distinct longitudinal gradient across the central U.S. with smaller (larger) values in the western (eastern) U.S. The ESI FD-INT is also relatively small across the western U.S., except for the northern tier of states. Together, these results reveal that unusually rapid decreases in SM and ET are more likely in humid areas with more vegetation. FD-INT is also large across most of the U. S for the SPI and SPEI; however, DRO-SEV is relatively less important across the eastern U.S. for these indicators. The relative importance of FD-INT for the SPI and SPEI shows that, though large precipitation deficits can develop quickly, it is difficult to maintain large deficits for an extended period of time, thereby leading to smaller DRO-SEV.

For EDDI, the average FD-INT is relatively large (small) across the western (eastern) U.S. The FD-INT and DRO-SEV terms together indicate that rapid increases in evaporative demand are more likely in the western U.S. whereas sustained periods of elevated evaporative demand are more likely in the southeastern U.S. (SEUS). Of all indicators evaluated during this study, EDDI has the highest flash drought occurrence across much of the U.S. Large maxima exceeding 8% of weeks cover wide swaths of the U.S. characterized by very different climates ranging from the arid desert Southwest to the semi-arid central High Plains and the moist and cool northeastern U.S. (NEUS). Though the structure of the EDDI flash drought occurrence pattern is very different than those of the ESI and SM in the western U.S., a similar pattern is seen in the SPEI and SPI in this region. This again indicates differences in flash drought detection when using meteorological and land surface indicators.

Inspection of the COMB statistics shows that the average FD-INT, DRO-SEV, and FDII associated with it are much smaller across most of the U.S. when compared to the single-variable indicators. The smaller COMB values are a consequence of its multivariate nature that averages contributions from multiple flash drought drivers and impacts into a single value. If flash drought signals are absent in one or more indicators, or cascade with time across different variables (Christian et al., 2020; Otkin et al., 2018), the value shown by COMB will be lower than the single-variable indicators because of differences in flash drought occurrence and peak severity. An advantage of COMB however is that greater confidence can be assigned to flash drought detections because at least two of the indicators must have an FDII >0 for the COMB FDII to be non-zero. The COMB FDII indicates that the strongest multivariate flash droughts occur across the central and SEUS, which is consistent with previous studies (Christian et al., 2019; Otkin et al., 2016) showing these regions to be susceptible to high-impact flash droughts. Despite having small average FDII, the COMB data set shows a high occurrence of flash drought across the U.S. and is an amalgam of the single-variable occurrence patterns. The high occurrence of COMB flash droughts in the western and northern U.S. is primarily due to the large number of EDDI and SPEI flash droughts. This leads to large differences across the northeastern and western U.S. where flash droughts are largely absent in the USDM. Though the EDDI values are probably too high (e.g., Ford et al., 2023), all indicators show that flash droughts occur in these regions, which suggests that the USDM may be too conservative depicting rapid drought intensification in the cooler NEUS and the arid and semi-arid western U.S. The less frequent USDM flash droughts could also reflect challenges associated with using a categorical drought index for flash drought identification.

### 4.3. Regional Flash Drought Analysis

In this section, we examine the multivariate characteristics of flash droughts for six regions of the U.S. (refer to Figure 1) that were chosen based on the geographic distribution of flash droughts in Figure 5 and regional differences in climate. Figure 6 shows the number of flash drought events and their maximum FDII averaged across all land grid points in each region. A flash drought for a given grid point and indicator is defined as a time period containing one or more consecutive weeks with an FDII > 0. Overall, there are some large differences between regions and indicators. In all regions except for the northwestern U.S. (NWUS), EDDI contains the most flash droughts; however, their average maximum FDII is generally lower than the other single-variable indicators. The

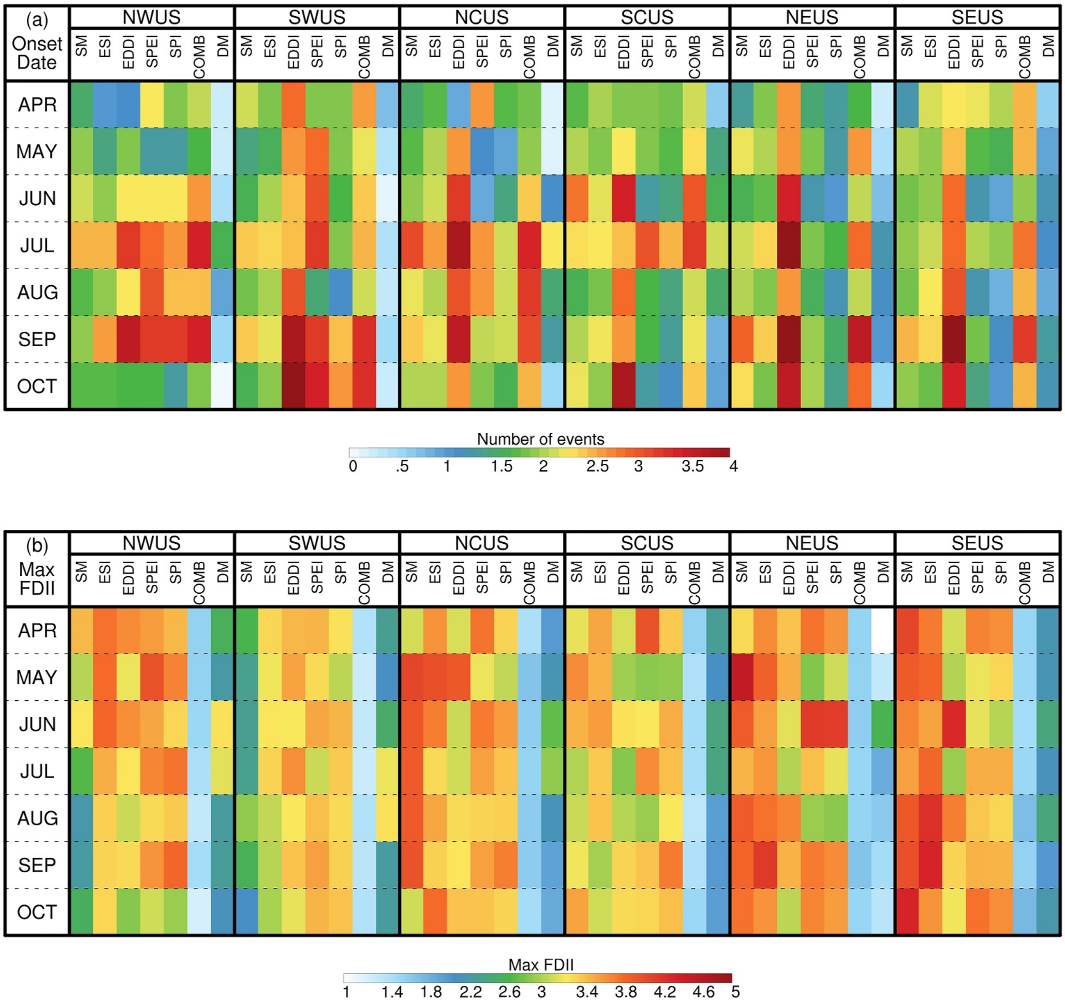


**Figure 7.** (a) Number of flash drought events that started in each month and their (b) maximum flash drought intensity index averaged across all land grid points for the soil moisture, Evaporative Stress Index, SPEI, EDDI, SPI, COMB, and USDM. The results are computed using weekly data during the 2001–2021 growing seasons (April–October) for the NWUS, SWUS, NCUS, SCUS, NEUS, and SEUS regions.

increase in the number of EDDI flash droughts relative to other indicators is largest for the NEUS where its use leads to around twice as many events. The fewest flash droughts are found in each region when using the USDM. The COMB data set has the second or third most events but the smallest average FDII in each region.

Another interesting feature of Figure 6 is that the central U.S. does not stand out as a flash drought hotspot when evaluated using the COMB data set despite its reputation as a prime area for flash drought. Most studies have used changes in SM or ESI to develop flash drought climatologies (Christian et al., 2019; Ford & Labosier, 2017; Otkin et al., 2021). These studies have found that flash droughts are most (least) common in the central and eastern (western) U.S., which is consistent with the SM and ESI results shown in this study. This pattern is also evident in the USDM, though it has fewer flash droughts overall. However, when meteorological data sets such as EDDI, SPI, and SPEI are used to identify flash drought, more events are found in the western U.S. than in the central U. S., which leads to more of the U.S. having a higher incidence of flash droughts.

To examine the seasonal characteristics of flash drought in each region, Figure 7 shows the number of flash droughts that started in each month along with the maximum FDII averaged over all grid points and events. For the NWUS, SM flash drought most often occurs during the first half of the growing season (May–July), whereas flash drought is more likely to begin in mid-summer to early fall in the other indicators. Despite having fewer flash droughts during the spring, these early season events tend to be stronger based on the maximum FDII. This

10.1029/2024WR037333

indicates that flash droughts that begin in the spring are more likely to persist and intensify during the summer due to the drier weather that prevails across the region during that time of the year. In contrast, the more numerous flash droughts that develop during the second half of summer tend to have lower FDII because there is less time for them to become severe before the return of cooler and wetter autumn weather. The USDM contains the fewest flash droughts, but like most indicators, identifies the majority of these events during the second half of the growing season with a peak in July.

For the southwestern U.S. (SWUS), the indicators show that flash drought onset occurs most often from July to October with a secondary maximum in April. Similar to the NWUS, the maximum in April is likely associated with an early onset of summer heat or the premature end to cool season precipitation. Flash droughts can develop at any time of the year according to the SPEI and EDDI. The seasonal pattern in flash drought occurrence indicates that flash droughts are often associated with poor summer monsoons that lead to flash drought onset during the latter half of summer into autumn. This hypothesis is supported by the maximum in the USDM FDII in July and August. There are also signals that land-atmosphere coupling processes may occur where rapid decreases in SM and ESI during late summer contribute to more intense heat waves and below normal rainfall in autumn, as indicated by the large number of EDDI, SPI, and SPEI flash droughts in September and October.

For the NCUS, flash drought onset occurs most frequently from July-September. Flash droughts during this time of the year can greatly reduce crop yields because the moisture stress associated with them occurs during critical stages for corn and soybean yield production (Jin et al., 2019; Otkin et al., 2016). In contrast, flash drought onset is more common from April to July across the SCUS, which is similar to the flash drought climatology presented in Christian et al. (2019). The tendency for flash droughts to develop earlier in the growing season in the SCUS is likely due to the importance of spring and early summer rainfall and the climatologically earlier onset of hot temperatures compared to areas further north. According to the SM and ESI, flash droughts in both regions are slightly more severe on average when they develop during the spring and early summer. Though EDDI often has the highest number of flash droughts in both regions, the average FDII associated with these events is relatively small, especially for the SCUS.

A distinct seasonal cycle in flash drought occurrence is not evident in the NEUS or SEUS. A notable feature for both regions is the high number of EDDI flash droughts relative to the other indicators. These events, however, tend to be relatively weak according to the FDII, especially for the SEUS, which indicates that rapid changes in evaporative demand are often not associated with rapid changes in land conditions. Similar to the central U.S., the average FDII for most indicators shows that flash droughts tend to be slightly more severe when their onset occurs during the first half of the growing season (April–June). According to the ESI and SM, severe flash droughts also occur later in the year (August–October) across the SEUS, which could be associated with a below normal tropical storm season. It also aligns with the occurrence of several high-impact flash droughts, such as the 2016 flash drought that increased wildfire risk and contributed to the devastating fires around Gatlinburg, TN (Case & Zavodsky, 2018).

## 5. Discussion

All flash droughts have two components: rapid intensification and sufficient duration to cause a drought impact (Otkin et al., 2018). Flash drought definitions, indicators, and monitoring tools developed over the past decade have largely focused on the rapid intensification component when characterizing flash drought, and less so on the cumulative severity of the event. However, impacts to agriculture, energy, and water resources are often caused by droughts with cumulative severity over multiple months (Stagge et al., 2015); it is less clear how the rate of intensification affects the frequency of severity of impacts (Otkin et al., 2022). Research has greatly advanced our understanding of the drivers of rapid drought intensification and the frequency with which it occurs (Christian et al., 2021; Mukherjee & Mishra, 2022; Nguyen et al., 2023; Osman et al., 2022; Yuan et al., 2023), but less is known about the drivers of flash drought persistence that can ultimately produce drought impacts of societal relevance. Our study is one of the first to comprehensively examine flash drought across the U.S. using a multivariate framework that considers both rapid intensification and cumulative severity. We find that the contributions of the rate of intensification and cumulative severity vary by drought indicator and region, which has implications for assessing the risk of flash drought impacts in any location. For example, unusually rapid intensification tends to produce larger responses in SM in the eastern U.S., whereas the cumulative severity of the flash drought tends to be more important for SM response in the western U.S. This suggests that rapid increases in precipitation deficits—as illustrated by SPI or SPEI—in the western U.S. may not be sufficient to produce drought impacts, and therefore the "flash" component of the hazard may be of less importance than the cumulative severity.

Additionally, most flash drought studies have characterized this multivariate hazard using a single indicator, often based on precipitation, ET, SM, or vegetation health (Lisonbee et al., 2021). Our findings show the fundamental characteristics of flash drought, including the frequency of occurrence, the severity, and the rate of intensification, are highly dependent on the flash drought indicator and the region in which that indicator is used. Similar evidence of strong indicator-dependence for flash drought has been shown by Osman et al. (2021) and Ford et al. (2023) among others; however our study is the first to demonstrate this important issue using a standardized framework with which to compare indicators (FDII). In this way, our study adds to the growing evidence supporting the need for multi-variable assessments of complex hazards like flash drought when determining climate-related water resource risks. Management strategies for flash drought should be developed on more holistic assessments of the hazard, including how meteorological drought conditions translate to socioeconomic and ecological impacts (Otkin et al., 2022).

The results of our study also illustrate regional differences in flash drought and its various impacts. While precipitation indicators preferentially identify flash droughts in the western U.S., these meteorological flash droughts do not translate to SM or vegetation impacts as effectively as in the eastern U.S. It is possible that vegetation stress in the western U.S. develops over longer time scales than those used in this study (Albano et al., 2020; Kannenberg et al., 2021). For example, Zhong et al. (2021) found the strongest, positive relationships between meteorological drought and vegetation response in the western U.S. over 2–6 months timescales. This suggests that current flash drought definitions focusing on rapid changes over a few weeks may need to be extended to changes occurring over longer timescales (e.g., seasonal) in more arid regions such as the western U.S. In addition, EDDI is the only meteorological drought indicator with an occurrence maximum across the NEUS, which appears to be unrealistic because drought itself was infrequent across the region during the study period (Chen et al., 2019). The high number of EDDI flash droughts may be a factor of how EDDI is derived (e.g., Ford et al., 2023), and not necessarily a robust flash drought signal. Meanwhile, meteorological anomalies tend to more effectively produce SM and/or vegetation response on subseasonal timescales in the central and eastern U.S., resulting in flash drought "hot spots" in these regions based on SM indicators (Ford & Labosier, 2017; Lowman et al., 2023). The results indicate that the DRO-SEV after the period of rapid intensification ends is a more important driver of the overall SM flash drought intensity than it is for the other data sets.

Regional differences in flash drought occurrence and severity could also be caused by our use of standardized change anomalies rather than percentiles to identify flash drought. Because an unusually rapid rate of intensification is the defining characteristic of flash drought, the thresholds used to determine this rate should account for the climatological variability at a given location. For example, for a location characterized by large temporal variability, a decline from above the 40th percentile to below the 20th percentile over two weeks—as is used in many flash drought definitions—may not be unusual. This means that use of percentile-based identification methods could result in erroneously large flash drought occurrence for locations with high variability, but too few flash droughts in regions with lower variability. Accounting for local variability via standardized change anomalies could lead to a stronger signal to noise ratio when identifying flash droughts across different regions and seasons.

## 6. Conclusions and Future Work

This study developed a multivariate flash drought climatology for the contiguous U.S. through application of the FDII framework to six widely used drought monitoring indicators that represent the meteorological drivers and surface impacts of drought. The FDII framework is useful because it considers both the rate of intensification and DRO-SEV when determining the strength of a flash drought. The flash drought climatology was developed using weekly data from the 2001–2021 growing seasons (April–October).

Overall, there are large differences in flash drought occurrence and severity depending upon which drought monitoring indicators are used to compute the FDII. The two precipitation indicators (SPI and SPEI) identified more flash droughts across the western U.S. whereas indicators of vegetation moisture stress (SM and ESI) identified more events in the central and eastern U.S. When assessed over the entire U.S., EDDI had the most flash droughts while the USDM had the fewest. Large differences were also evident in the relative importance of the

FD-INT and DRO-SEV terms for different regions and indicators. For example, the severity of SPI and SPEI flash droughts was more strongly influenced by how quickly the precipitation deficits developed rather than by the size of the subsequent deficits. Similar behavior occurred for EDDI across parts of the western and northern U.S. where flash DRO-SEV was more closely related to how quickly the evaporative demand increased. Evaluation of the SM and ESI data sets revealed a distinct longitudinal gradient in intensification rates, with larger values in the central and eastern U.S. It was also shown that the magnitude of the drought conditions after the rapid intensification ends is a key driver of flash DRO-SEV in the more humid central and eastern U.S. When the COMB data set was used, the strongest multivariate flash droughts were located in the central and SEUS. Together, these results illustrate the need to use a multivariate assessment framework to identify flash droughts and to characterize their severity.

The seasonal analysis of flash drought occurrence and severity revealed several notable differences between regions and data sets. A distinct seasonal cycle in flash drought occurrence was evident in the western and central U.S. regions but was not as apparent in the eastern U.S. Overall, flash droughts occurred more often from June-September in the NWUS, July-October in the SWUS, July-September in the NCUS, and April-July in the SCUS. According to the ESI, flash droughts are less common but more severe when they develop during the spring. Severe SM and ESI flash droughts also frequently develop across the SEUS during autumn.

Future studies will investigate the potential impact of various physical drivers, such as the North American Monsoon, tropical cyclones, and anomalous large-scale circulation patterns, on the occurrence and severity of flash drought across different parts of the U.S. We also plan to modify the FDII so that it can be used in real-time drought monitoring systems. The current version of the FDII is optimized to work with data sets containing complete time series where the onset and maximum severity of a flash drought can be readily determined. For real-time monitoring, changes will need to be made to the FDII because only the FD-INT term can be computed during the initial stages of a flash drought. Alternative formulations such as the rapid change index (Otkin et al., 2014) could also be used to assess the magnitude of the rapid intensification. Likewise, the DRO-SEV term could be modified so that it represents the cumulative DRO-SEV up to the current date rather than the average severity over a longer time period for which data is not yet available. Additional experiments could be performed to assess the sensitivity of the FD-INT, DRO-SEV, and FDII to different baseline intensification rate and DRO-SEV thresholds. It would also be beneficial to extend the FDII framework to include hydrological variables such as streamflow, reservoir levels, and snow water equivalent to obtain additional information about the impact of flash drought on water resource availability. Together, these future studies will promote efforts to improve understanding of flash droughts and the comprehensive monitoring of their evolution, both of which will aid development of robust drought early warning systems.

## Data Availability Statement

All of the following data sets used in this study are publicly available: NLDAS2 SM (https://hydro1.gesdisc.eosdis.nasa.gov/data/NLDAS/NLDAS_NOAH0125_H.002/), EDDI (https://psl.noaa.gov/eddi/), ESI (https://climateserv.servirglobal.net/map), and USDM (https://droughtmonitor.unl.edu/CurrentMap.aspx). SPI and SPEI data are available through Ford et al. (2023). The multivariate FDII data sets generated during this project are accessible via zenodo at https://zenodo.org/records/12702004. (Otkin et al., 2024).

**Acknowledgments**
The authors acknowledge support provided by the NOAA Climate Program Office Modeling, Analysis, Predictions, and Projections program under Grants NA22OAR4310137 and NA22OAR4310135.

## References

Abatzoglou, J. T. (2013). Development of gridded surface meteorological data for ecological applications and modeling. *International Journal of Climatology*, *33*(1), 121–131. https://doi.org/10.1002/joc.3413

Albano, C. M., McGwire, K. C., Hausner, M. B., McEvoy, D. J., Morton, C. G., & Huntington, J. L. (2020). Drought sensitivity and trends of riparian vegetation vigor in Nevada, USA (1985-2018). *Remote Sensing*, *12*(9), 1362. https://doi.org/10.3390/rs12091362

Allen, R. G., Pereira, L. S., Raes, D., & Smith, M. (1998). Crop evapotranspiration – Guidelines for computing crop water requirements. In *FAO irrigation and drainage paper, No. 56*. FAO.

Anderson, M. C., Norman, J. M., Diak, G. R., Kustas, W. P., & Mecikalski, J. R. (1997). A two-source time-integrated model for estimating surface fluxes using thermal infrared remote sensing. *Remote Sensing of Environment*, *60*(2), 195–216. https://doi.org/10.1016/S0034-4257(96)00215-5

Anderson, M. C., Norman, J. M., Mecikalski, J. R., Otkin, J. A., & Kustas, W. P. (2007a). A climatological study of fluxes and moisture stress across the continental U. S. based on thermal remote sensing. 1: Model formulation. *Journal of Geophysical Research*, *112*(D10), D10117. https://doi.org/10.1029/2006JD007506

Anderson, M. C., Norman, J. M., Mecikalski, J. R., Otkin, J. A., & Kustas, W. P. (2007b). A climatological study of evapotranspiration and moisture stress across the continental U.S. Based on thermal remote sensing: 2. Surface moisture climatology. *Journal of Geophysical Research*, *112*(D11), D11112. https://doi.org/10.1029/2006JD007507

Barlage, M., Chen, F., Tewari, M., Ikeda, K., Gochis, D., Dudhia, J., et al. (2010). Noah land surface model modifications to improve snowpack prediction in the Colorado Rocky Mountains. *Journal of Geophysical Research*, *115*(D22), D22101. https://doi.org/10.1029/2009JD013470

Case, J. L., & Zavodsky, B. T. (2018). Evolution of 2016 drought in the Southeastern United States from a land surface modeling perspective. *Results in Physics*, *8*, 654–656. https://doi.org/10.1016/j.rinp.2017.12.029

Chen, L. G., Gottschalck, J., Hartman, A., Miskus, D., Tinker, R., & Artusa, A. (2019). Flash drought characteristics based on U.S. Drought Monitor. *Atmosphere*, *10*(9), 498. https://doi.org/10.1016/j.rinp.2017.12.029

Christian, J., Hobbins, M., Hoell, A., Otkin, J. A., Ford, T., Cravens, A., et al. (2024). Flash drought: A state of the science review. *WIREs Water*, *11*(3), e1714. https://doi.org/10.1002/wat2.1714

Christian, J. I., Basara, J. B., Hunt, E. D., Otkin, J. A., Furtado, J. C., Mishra, V., et al. (2021). Global distribution, trends, and drivers of flash drought occurrence. *Nature Communications*, *12*(1), 6330. https://doi.org/10.1038/s41467-021-26692-z

Christian, J. I., Basara, J. B., Hunt, E. D., Otkin, J. A., & Xiao, X. (2020). Flash drought development and cascading impacts associated with the 2010 Russian heatwave. *Environmental Research Letters*, *15*(9), 094078. https://doi.org/10.1088/1748-9326/ab9faf

Christian, J. I., Basara, J. B., Otkin, J. A., Hunt, E. D., Wakefield, R. A., Flanagan, P. X., & Xiao, X. (2019). A methodology for flash drought identification in gridded datasets: Application of flash drought frequency across the United States. *Journal of Hydrometeorology*, *20*(5), 833–846. https://doi.org/10.1175/JHM-D-18-0198.1

Christian, J. I., Martin, E. R., Basara, J. B., Furtado, J. C., Otkin, J. A., Lowman, L. E., et al. (2023). Global projections of flash drought in a warming climate. *Communications Earth and Environment*, *4*(1), 165. https://doi.org/10.1038/s43247-023-00826-1

Daly, C., Halbleib, M., Smith, J. I., Gibson, W. P., Doggett, M. K., Taylor, G. H., et al. (2008). Physiographically-sensitive mapping of temperature and precipitation across the conterminous United States. *International Journal of Climatology*, *28*(15), 2031–2064. https://doi.org/10.1002/joc.1688

Ek, M. B., Mitchell, K. E., Lin, Y., Rogers, P., Grunmann, P., Koren, V., et al. (2003). Implementation of Noah land surface model advances in the National Centers for Environmental Prediction operational mesoscale Eta model. *Journal of Geophysical Research*, *108*(D22), 8851. https://doi.org/10.1029/2002JD003296

Ford, T. W., & Labosier, C. F. (2017). Meteorological conditions associated with the onset of flash drought in the eastern United States. *Agriculture and Forest Meteorology*, *247*, 414–423. https://doi.org/10.1016/j.agrformet.2017.08.031

Ford, T. W., Otkin, J. A., Quiring, S. M., Lisonbee, J., Woloszyn, M., Wang, J., & Zhong, Y. (2023). Flash drought indicator inter-comparison: A focus on flash drought monitoring in the United States [Dataset]. *Journal of Applied Meteorology and Climatology*, *62*(12), 1713–1730. https://doi.org/10.1175/JAMC-D-23-0081.1

Ford, T. W., & Quiring, S. (2019). Comparison of contemporary in situ, model, and satellite remote sensing soil moisture with a focus on drought monitoring. *Water Resources Research*, *55*(2), 1565–1582. https://doi.org/10.1029/2018WR024039

Hobbins, M. T., Wood, A., McEvoy, D. J., Huntington, J. L., Morton, C., Anderson, M., & Hain, C. (2016). The Evaporative Demand Drought Index. Part I: Linking drought evolution to variations in evaporative demand. *Journal of Hydrometeorology*, *17*(6), 1745–1761. https://doi.org/10.1175/JHM-D-15-0121.1

Hoell, A., Parker, B. A., Downey, M., Umphlett, N., Jencso, K., Akyuz, F. A., et al. (2020). Lessons learned from the 2017 flash drought across the US northern great Plains and Canadian prairies. *Bulletin of the American Meteorological Society*, *101*(12), E2171–E2185. https://doi.org/10.1175/BAMS-D-19-0272.1

Hoerling, M., Eischeid, J., Kumar, A., Leung, R., Mariotti, A., Mo, K., et al. (2014). Causes and predictability of the 2012 great Plains drought. *Bulletin of the American Meteorological Society*, *95*(2), 269–282. https://doi.org/10.1175/BAMS-D-13-00055.1

Hunt, E., Femia, F., Werrell, C., Christian, J. I., Otkin, J. A., Basara, J., et al. (2021). Agricultural and food security impacts from the 2010 Russia flash drought. *Weather and Climate Extremes*, *34*, 100383. https://doi.org/10.1016/j.wace.2021.100383

Jin, C., Luo, X., Xiao, X., Dong, J., Li, X., Yang, J., & Zhao, D. (2019). The 2012 flash drought threatened US Midwest agroecosystems. *Chinese Geographical Science*, *29*(5), 768–783. https://doi.org/10.1007/s11769-019-1066-7

Kannenberg, S. A., Driscoll, A. W., Malesky, D., & Anderegg, W. R. L. (2021). Rapid and surprising dieback of Utah juniper in the southwestern USA due to acute drought stress. *Forest Ecology and Management*, *480*, 118639. https://doi.org/10.1016/j.foreco.2020.118639

Koster, R. D., Schubert, S. D., Wang, H., Mahanama, S. P., & DeAngelis, A. M. (2019). Flash drought as captured by reanalysis data: Disentangling the contributions of precipitation deficit and excess evapotranspiration. *Journal of Hydrometeorology*, *20*(6), 1241–1258. https://doi.org/10.1175/JHMD-18-0242.1

Li, J., Wang, Z., Wu, X., Chen, J., Guo, S., & Zhang, Z. (2020). A new framework for tracking flash drought events in space and time. *CATENA*, *194*, 104763. https://doi.org/10.1016/j.catena.2020.104763

Liang, M., Yuan, X., Zhou, S., & Ma, Z. (2023). Spatiotemporal evolution and nowcasting of the 2022 Yangtze River mega-flash drought. *Water*, *15*, 2744. https://doi.org/10.3390/w15152744

Lisonbee, J., Woloszyn, M., & Skumanich, M. (2021). Making sense of flash drought: Definitions, indicators, and where we go from here. *Journal of Applied Service Climatology*, *2021*, 1–19. https://doi.org/10.46275/joasc.2021.02.001

Liu, Y., Zhu, Y., Zhang, L., Ren, L., Yuan, F., Yang, X., & Jiang, S. (2020). Flash droughts characterization over China: From a perspective of the rapid intensification rate. *Science of the Total Environment*, *704*, 135373. https://doi.org/10.1016/j.scitotenv.2019.135373

Lowman, L. E. L., Christian, J. I., & Hunt, E. D. (2023). How land surface characteristics influence the development of flash drought through the drivers of soil moisture and vapor pressure deficit. *Journal of Hydrometeorology*, *24*(9), 1395–1415. https://doi.org/10.1175/JHM-D-22-0158.1

Mahto, S. S., & Mishra, V. (2023). Increasing risk of simultaneous occurrence of flash drought in major global croplands. *Environmental Research Letters*, *18*(4), 044044. https://doi.org/10.1088/1748-9326/acc8ed

McKee, T. B., Doesken, N. J., & Kleist, J. (1993). The relationship of drought frequency and duration to time scales. In *Eighth conference on applied climatology*. Anaheim.

Mishra, V., Aadhar, S., & Mahto, S. S. (2021). Anthropogenic warming and intraseasonal summer monsoon variability amplify the risk of future flash droughts in India. *npj Climate and Atmospheric Science*, *4*(1), 1. https://doi.org/10.1038/s41612-020-00158-3

Mohammadi, K., Jiang, Y., & Wang, G. (2022). Flash drought early warning based on the trajectory of solar-induced chlorophyll fluorescence, *Proceedings of the national academy of Sciences* (Vol. 119(32)). https://doi.org/10.1073/pnas.2202767119

Mukherjee, S., & Mishra, A. K. (2022). A multivariate flash drought indicator for identifying global hotspots and associated climate controls. *Geophysical Research Letters*, *49*(2). https://doi.org/10.1029/2021GL096804

Nguyen, H., Wheeler, M. C., Hendon, H. H., Lim, E.-P., & Otkin, J. A. (2021). The 2019 flash droughts in subtropical eastern Australia and their association with large-scale climate drivers. *Weather and Climate Extremes*, *32*, 100321. https://doi.org/10.1016/j.wace.2021.100321

Nguyen, H., Wheeler, M. C., Otkin, J. A., Frost, A., Stone, R., & Cowan, T. (2019). Using the evaporative stress index to monitor flash drought in Australia. *Environmental Research Letters*, *14*(6), 064016. https://doi.org/10.1088/1748-9326/ab2103

Nguyen, H., Wheeler, M. C., Otkin, J. A., Nguyen-Huy, T., & Cowan, T. (2023). Climatology and composite evolution of flash drought over Australia and its vegetation impacts. *Journal of Hydrometeorology*, *24*(6), 1087–1101. https://doi.org/10.1175/JHM-D-22-0033.1

Noguera, I., Domínguez-Castro, F., & Vicente-Serrano, S. M. (2020). Characteristics and trends of flash droughts in Spain, 1961–2018. *Annals of the New York Academy of Sciences*, *1472*(1), 155–172. https://doi.org/10.1111/nyas.14365

Norman, J. M., Kustas, W. P., & Humes, K. S. (1995). A two-source approach for estimating soil and vegetation energy fluxes from observations of directional radiometric surface temperature. *Agriculture and Forest Meteorology*, *77*, 263–292. https://doi.org/10.1016/0168-1923(95)02265-Y

Osman, M., Zaitchik, B., Badr, H., Otkin, J. A., Zhong, Y., Lorenz, D., et al. (2022). Diagnostic classification of flash drought events reveals distinct classes of forcings and impacts. *Journal of Hydrometeorology*, *23*(2), 275–289. https://doi.org/10.1175/JHM-D-21-0134.1

Osman, M., Zaitchik, B. F., Badr, H. S., Christian, J., Tadesse, T., Otkin, J. A., & Anderson, M. C. (2021). Flash droughts over the contiguous United States: Sensitivity of inventories and trends to quantitative definitions. *Hydrology and Earth System Sciences*, *25*(2), 565–581. https://doi.org/10.5194/hess-25-565-2021

Otkin, J. A., Anderson, M. C., Hain, C., Mladenova, I., Basara, J., & Svoboda, M. (2013). Examining rapid onset drought development using the thermal infrared based Evaporative Stress Index. *Journal of Hydrometeorology*, *14*(4), 1057–1074. https://doi.org/10.1175/JHM-D-12-0144.1

Otkin, J. A., Anderson, M. C., Hain, C., & Svoboda, M. (2014). Examining the relationship between drought development and rapid changes in the evaporative stress index. *Journal of Hydrometeorology*, *15*(3), 938–956. https://doi.org/10.1175/JHM-D-13-0110.1

Otkin, J. A., Anderson, M. C., Hain, C., Svoboda, M., Johnson, D., Mueller, R., et al. (2016). Assessing the evolution of soil moisture and vegetation conditions during the 2012 United States flash drought. *Agriculture and Forest Meteorology*, *218–219*, 230–242. https://doi.org/10.1016/j.agrformet.2015.12.065

Otkin, J. A., Svoboda, M., Hunt, E. D., Ford, T. W., Anderson, M. C., Hain, C., & Basara, J. B. (2018). Flash droughts: A review and assessment of the challenges imposed by rapid-onset droughts in the United States. *Bulletin of the American Meteorological Society*, *99*(5), 911–919. https://doi.org/10.1175/BAMS-D-17-0149.1

Otkin, J. A., Woloszyn, M., Wang, H., Svoboda, M., Skumanich, M., Pulwarty, R., et al. (2022). Getting ahead of flash drought: From early warning to early action. *Bulletin of the American Meteorological Society*, *103*(10), E2188–E2202. https://doi.org/10.1175/BAMS-D-21-0288.1

Otkin, J. A., Zhong, Y., Ford, T. W., Anderson, M. C., Hain, C., Hoell, A., et al. (2024). Multivariate flash drought intensity index datasets [Dataset]. *Zenodo*. https://doi.org/10.5281/zenodo.12702004

Otkin, J. A., Zhong, Y., Hunt, E. D., Christian, J. I., Basara, J. B., Nguyen, H., et al. (2021). Development of a flash drought intensity index. *Atmosphere*, *12*(6), 741. https://doi.org/10.3390/atmos12060741

Parker, T., Gallant, A., Hobbins, M., & Hoffmann, D. (2021). Flash drought in Australia and its relationship to evaporative demand. *Environmental Research Letters*, *16*(6), 064033. https://doi.org/10.1088/1748-9326/abfe2c

Pendergrass, A. G., Meehl, G. A., Pulwarty, R., Hobbins, M., Hoell, A., AghaKouchak, A., et al. (2020). Flash droughts present a new challenge for subseasonal-to-seasonal prediction. *Nature Climate Change*, *10*(3), 191–199. https://doi.org/10.1038/s41558-020-0709-0

Stagge, J. H., Kohn, I., Tallaksen, L. M., & Stahl, K. (2015). Modeling drought impact occurrence based on meteorological drought indices in Europe. *Journal of Hydrology*, *530*, 37–50. https://doi.org/10.1016/j.jhydrol.2015.09.039

Svoboda, M., LeComte, D., Hayes, M., Heim, R., Gleason, K., Angel, J., et al. (2002). The drought monitor. *Bulletin of the American Meteorological Society*, *83*(8), 1181–1190. https://doi.org/10.1175/1520-0477-83.8.1181

Vicente-Serrano, S. M., Begueria, S., & Lopez-Moreno, J. I. (2010). A multiscalar drought index sensitive to global warming: The standardized precipitation evapotranspiration index. *Journal of Climate*, *23*(7), 1696–1718. https://doi.org/10.1175/2009JCLI2909.1

Wang, Y., & Yuan, X. (2021). Anthropogenic speeding up of south China flash droughts as exemplified by the 2019 summer-autumn transition season. *Geophysical Research Letters*, *48*, 1–9. https://doi.org/10.1029/2020GL091901

Wei, H., Xia, Y., Mitchell, K. E., & Ek, M. B. (2013). Improvement of the Noah land surface model for warm season processes: Evaluation of water and energy flux simulation. *Hydrological Processes*, *27*(2), 297–303. https://doi.org/10.1002/hyp.9214

Xia, Y., Mitchell, K., Ek, M., Sheffield, J., Cosgrove, B., Wood, E., et al. (2012). Continental-scale water and energy flux analysis and validation of the North American land data assimilation system project phase 2 (NLDAS-2): 1. Intercomparison and application of model products. *Journal of Geophysical Research*, *117*(D3), D03110. https://doi.org/10.1029/2011JD016048

Yuan, X., Wang, Y., Ji, P., Sheffield, J., & Otkin, J. A. (2023). A global transition to flash droughts under climate change. *Science*, *380*(6641), 187–191. https://doi.org/10.1126/science.abn6301

Zhong, S., Sun, Z., & Liping, D. (2021). Characteristics of vegetation response to drought in the CONUS based on long-term remote sensing and meteorological data. *Ecological Indicators*, *127*, 107767. https://doi.org/10.1016/j.ecolind.2021.107767

Zscheischler, J., Westra, S., van den Hurk, B. J. J. M., Seneviratne, S. I., Ward, P. J., Pitman, A., et al. (2018). Future climate risk from compound events. *Nature Climate Change*, *8*(6), 469–477. https://doi.org/10.1038/s41558-018-0156-3